

Research Article

A Novel Numerical Model for Simulating the Quantity of Tailing Oil in the Mixed Segment between Two Batches in Product Pipelines

Guoxi He ¹, Na Yang,¹ Kexi Liao ¹, Baoying Wang,² and Liying Sun¹

¹CNPC Key Laboratory of Oil & Gas Storage and Transportation, Petroleum Engineering School, Southwest Petroleum University, Chengdu 610500, China

²Beijing Key Laboratory of Urban Oil and Gas Distribution Technology, China University of Petroleum-Beijing, Beijing 102249, China

Correspondence should be addressed to Guoxi He; heguoxicup@163.com and Kexi Liao; liaokxswpi@163.com

Received 21 March 2019; Revised 26 May 2019; Accepted 30 July 2019; Published 19 August 2019

Academic Editor: Arkadiusz Zak

Copyright © 2019 Guoxi He et al. This is an open access article distributed under the Creative Commons Attribution License, which permits unrestricted use, distribution, and reproduction in any medium, provided the original work is properly cited.

Cutting mixed oil in product pipelines has a great influence on the economy of the pipeline operation processes. The reasonable prediction of CDMS (the concentration distribution in the mixed segment) is important for cutting mixed segments. The classical model cannot explain the tailing phenomenon well which should not be neglected during operation processes. Based on Fick's diffusion law, a new model for calculating the diffusion coefficient is proposed in this article, which originates from the essence of the diffusion phenomenon and considers the effects of both physical properties of oil products and the turbulence. At the same time, the dynamic fluid equilibrium model of CDMS near the pipe wall is given which has considered the adsorption effect of wall roughness. Based on these two factors, a novel numerical model for simulating the quantity of tailing oil is proposed, which is solved via the characteristic method and the finite difference method. The effects of different physical properties, as well as the adsorption, on both LFMS (the length of the front of the mixed segment) and LTMS (the length of the tail of the mixed segment), are analyzed. The comparison between the simulation results and the experimental data is utilized to validate the proposed numerical model. The simulation results show that the novel model can well describe the mixed segment tailing phenomenon and also explain the mixing essence of two miscible but dissimilar fluids in the pipeline more clearly. To sum up, this model can provide theoretical guidance for the prediction of CDMS and cutting process in practical operation processes; therefore, more economic benefit can be obtained.

1. Background

Sequential transportation of multiproduct pipelines is a process by which refined oils are transported continuously with a certain sequence in the pipeline, as shown in Figure 1. When the oil is transported alternately, because of the lack of isolation, the mixed oil will be inevitably generated [1]. With the increase in transportation time and distance, CDMS will change gradually [2]. The fluid physical properties and the corresponding quality indicators in LMS will also change [3–5].

During the process of batch transportation, mixed oil is influenced by heat, mass, and momentum transfer concurrently

[6, 7]. The mixed oil develops continuously in the axial direction. Resulting from the comprehensive effect of heat, mass, and momentum transfer among different products during the transportation process, the formation of mixed oil is based on convection transfer and diffusion transfer [8–10], as can be seen in Figure 1.

The calculation method of the oil mixture is divided into the theoretical formula and empirical formula. The mixing quantity of the mixed segment between two batches is calculated directly by the empirical formula. Among the previous studies, the empirical formula proposed by American scholars Austin and Palfery [12] is the most widely adopted one to engineering prediction of LMS, which shows

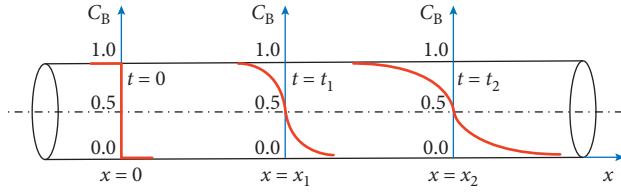


FIGURE 1: Characterization of the mixing process at a different distance and different time (convection and diffusion) [11].

that LMS is related to the inner diameter of the pipe, the Reynolds number, the viscosity of the two batches, and the calculated length of the pipe segment. Austin and Palfery [12] also pointed out that there was a critical Reynolds number which had a significant influence on the increasing LMS. In addition, some other empirical formulas [13–18] are given in the form of the ratio of the mixed segment to pipeline volume. It is found that the mixed segment is related to the calculated length of the pipeline [13–16], the inner diameter of the pipeline [13–15,17], the Reynolds number [13, 14], the oil density and viscosity [15, 16], the volume fraction [13], and the concentration coefficient Z value [14, 17] during the mixed segment transporting in the pipeline. Here, $Z = x / (2\sqrt{D_{\text{axial}}t})$, where x is the axial distance from the beginning of the pipe (m), t is the time (s), and D_{axial} is the effective axial diffusion coefficient (m^2/s). It is noticed that Z is the concentration coefficient of front oil to determine the cutting point on the concentration curve (dimensionless). In the specific mathematical formula, Z is the independent variable in the Gauss error function.

Convection-diffusion equation is a theoretical formula used to solve the governing equation of the concentration curve in the mixed segment. The convection-diffusion equation is established by convection and diffusion effects which are the two most important factors affecting the mixed segment. The convection-diffusion equations are mostly 3D but can be reduced to 1D or 2D depending on geometry or as a result of simplifications. The one-dimensional equation considers that the concentration and the velocity are constant in the pipe cross section and are independent of the radial position. The two-dimensional equation can better describe the mixed phenomenon, and its calculation is relatively accurate. But it is relatively difficult to perform the calculation in a long-distance pipeline at the same time. The diffusion coefficient is very important to calculate the mixed segment in the diffusion term. Empirical formulas are often used to calculate the effective diffusion coefficients in one-dimensional equations, which are also applied together with turbulent diffusion coefficients to two-dimensional models.

It is widely believed that the effective diffusion coefficient is related to the Re number [13, 18], oil viscosity [13, 14, 16, 17], pipeline length [13, 15, 17], pipeline diameter [13, 15, 17], oil density during the sequential transportation process [13], friction coefficient [18], Fowler–Brown coefficient [15], etc. For the two-dimensional model, the diffusion coefficient is divided into the molecular diffusion

coefficient and turbulent diffusion coefficient. The molecular diffusion coefficient is usually fixed and only considered in the bottom layer and the buffer layer in turbulent flow or in the totally laminar pipe flow. The turbulent diffusion coefficient is calculated by the corresponding empirical formula in the core region of the turbulent pipe flow. Some scholars believe that the turbulent diffusion coefficient is related to the calculated length of the pipeline [13, 15, 17], the inner diameter of the pipeline [13, 15, 17], the friction coefficient [13, 18], the average flow velocity in the pipeline, the average viscosity of the two oils, and the Reynolds number corresponding to the average viscosity [13, 14, 16, 17].

However, when using the empirical formula or the convection-diffusion equation to solve the mixed segment, it is the average values of the density, viscosity, and temperature of the two oils that are used to solve the model. When these empirical formulas are used to calculate the mixed segment, the sequence of transportation has no influence on the calculated volume of the mixed segment. However, it is found in the engineering practice that, with the same parameters, the mixture quantity of gasoline followed by diesel is smaller than that of diesel followed by gasoline. When diesel is followed by gasoline, diesel will adhere to the pipe wall more firmly, which leads to a harder work for gasoline to replace diesel by continual scouring. On the wall of the pipeline, the replacement process of the oil at the tail of LMS is slowing down, resulting in an increase of LTMS. The existing models cannot describe the influence of the oil sequence on mixed segment quantity and distribution nor can describe the phenomenon of mixed segment trailing. The above are the factors influencing the mixed segment in the theoretical and empirical formulas. In addition, some engineering factors may also affect the mixed oil, including mixed oil trailing, the unstable quality potential of oil source products, the variable demand of pipeline transportation changing with the market, the possession of mixed oil tank capacity, the limitation of oil mixing, and other factors. In order to improve the accuracy of mixed segment prediction, this paper describes the trailing phenomenon of the mixed segment, considers the difference in physical properties of oil products at the front and tail of the mixed segment, and takes the influence of the pipe wall adsorption on CDMS into consideration.

The contribution and innovation of this paper are as follows: (1) A novel model is proposed to simulate CDMS, which takes into account the turbulence effect, the difference of the physical properties of the fluid, and the adsorption effect of the pipe wall roughness. The novel model holds a new diffusion coefficient. (2) Sensitivity analysis is carried out on the key factors affecting the quantity of mixed oil as well as LTMS and LFMS.

2. Numerical Modeling of Interfacial Mixing: Mass Transfer Equation

2.1. One-Dimensional Convection-Diffusion Equation. Taylor [14] believes that when the mixed segment passes slowly through a small-diameter pipe, it will spread across the cross section under the combined action of molecular diffusion and

velocity change. Moreover, although the flow is not symmetric, the concentration distribution produced in this manner is symmetric. The one-dimensional mixing model considers that the oil concentration in the pipeline radial direction is uniform and only considers the change of the oil concentration in the axial direction. The one-dimensional model adopts the effective axial diffusion coefficient D_{axial} [19, 20] to reflect the comprehensive degree of diffusion when the diffusion term is simplified. The coefficient can reflect the comprehensive influence of the extension and growth of the mixed segment along the pipeline [19]. The one-dimensional convection-diffusion equation is obtained on the basis of Fick's diffusion law and mass conservation equation [20, 21]:

$$\frac{\partial C}{\partial t} + u_m \frac{\partial C}{\partial x} = D_{\text{axial}} \frac{\partial^2 C}{\partial x^2}. \quad (1)$$

Here, it is noticed that $D_{\text{axial}} = 5.05 d \sqrt{\tau_0 / \rho}$, $\tau_0 = 0.125 \lambda \rho u_m^2$, and $\lambda = 0.3164 \text{Re}^{-0.25}$ when using the Blasius correlation for turbulent flow in smooth pipes up to $\text{Re} = 10^5$. C is the average volume concentration of product B in the mixed segment (dimensionless), u_m is the average velocity at the cross-sectional area of the mixed segment (m/s), D_{axial} is the effective axial diffusion coefficient (m^2/s), t is the time (s), x is the axial distance from the beginning of the pipe (m), d is the inner diameter of the pipe (m), τ_0 is the wall shear stress (Pa), and ρ is the average density of the oil (kg/m^3).

2.2. Two-Dimensional Convection-Diffusion Equation. Aunicky [13] argues that the Taylor [14] model is not entirely satisfactory because the diffusion coefficient D_{axial} increases with the length of the pipe rather than being a constant. The two-dimensional convection-diffusion equation can simultaneously take the axial and radial change of oil concentration into consideration. Because of the particular shape of the pipe, the cylindrical coordinate equation is used to solve the equation, the basic form of which is as follows, which is under the assumption of one-dimensional flow in the axial direction and axial symmetry for diffusion:

$$\frac{\partial C}{\partial t} + u_m \frac{\partial C}{\partial x} = \frac{1}{r} \cdot \frac{\partial}{\partial r} \left(r D_{\text{axial}} \frac{\partial C}{\partial r} \right) + \frac{\partial}{\partial x} \left(D_{\text{axial}} \frac{\partial C}{\partial x} \right). \quad (2)$$

Here, the definitions of the variables are the same as before.

3. Diffusion Coefficient and Adsorption Effects of the Pipe Wall

3.1. Turbulent Diffusion Coefficient. In order to minimize the quantity of mixed oil formed in the process of refined oil batch transportation and to enhance the economy of pipeline operation, the pipeline for sequential transportation requires a turbulent flow state. The turbulent flow in a circular tube contains momentum exchange between different flow layers, which makes the velocity distribution in the center of the pipe more uniform. The laminar region is close to the wall. The center region is located where turbulence is fully developed. The buffer region is between laminar flow and fully developed turbulent flow. The two-

dimensional convection-diffusion equation can be simplified differently in different regions according to different oil-mixing mechanisms. The specific division of different regions is shown in Figure 2 [15].

During the mixing process, the flow regime has a great impact on the volume of mixed oil. More uniform velocity distribution in the central portion of the pipe is resulted from the momentum exchange between different flow layers caused by the pulsation. Because of the restriction of the pipe wall, the pulsation is completely eliminated near the pipe wall. Table 1 simplifies the formulas for different regions. In the table, R is the radius of the tube (m); r is the distance away from the tube center in the radial direction (m); y is the distance away from the tube wall in the radial direction, and $y = R - r$ (m); D_{mole} is the molecular diffusion coefficient (m^2/s); D_{turb} is the turbulent diffusion coefficient, which can reflect the effect of turbulence on the diffusion coefficient (m^2/s); and ν is the fluid kinematic viscosity (m^2/s).

3.2. Effects of the Difference in Density and Viscosity on the Adjacent Segment. Tichacek et al. [18] modified the analysis method of Taylor [14] and analyzed the axial mixing problem in the straight pipe. They found that when the fluid was close to the laminar flow regime, the axial mixing increased rapidly. At the same time, the roughness of the pipe could also lead to a small quantity of the axial mixed segment, while the kinematic viscosity of the pipe would not change greatly from one area to another. According to Freitas et al. [8], under the action of radial diffusion, the axial distribution of the mixed segment becomes more compact and the axial extension is also inhibited. So the quantity of VMS in the turbulent state is much less than that in the laminar flow state. In addition, the reason for mixing is also related to the viscosity and density of the two oil products in sequential transportation. Freitas et al. [8] established the oil-mixing estimation model, which took into account the influence of viscosity change on the mixed segment. The variations in viscosity can promote changes in concentration as well as the bulk-average fluid velocity which is capable of altering substantially the Reynolds number and Schmidt number. Such a variation could induce a significant change in the effective axial dispersion coefficient and, consequently, in the mixing volume. The flow rate used in their model changes over time and diameter as well as the concentration of the mixed segment, which makes the model more accurate. Lulie [22] believed that when the temperature field has great fluctuations along the pipeline, the difference in density and viscosity of the adjacent oil is an important factor affecting the formation of the mixed segment, and the velocity field in the mixed segment area changes gradually. The velocity profile in the mixed zone changes gradually and is different from that in the homogeneous zone.

Suppose that, in the beginning, only oil A with a density of ρ_1 and a viscosity of μ_1 flows in the pipe. Then, inject oil B is miscible with oil A and has a density of ρ_2 and a viscosity of μ_2 . Under turbulent conditions, the difference in density between adjacent oils is much smaller than that in the

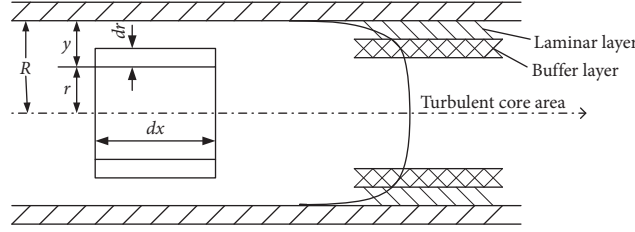


FIGURE 2: Division of the flow area in a pipeline.

TABLE 1: Simplified formulas of the flow regions [19, 20].

Region	Distance to the pipe wall	Velocity distribution	Turbulent diffusion coefficient	Effective axial diffusion coefficient
Laminar layer	$y < (5\nu/\sqrt{\tau_0/\rho})$	$u = \tau_0 y/\rho\nu$	$D_{\text{turb}} = 0$	$D_{\text{axial}} = D_{\text{mole}}$
Buffer layer	$(5\nu/\sqrt{\tau_0/\rho}) \leq y \leq (30\nu/\sqrt{\tau_0/\rho})$	$u = \sqrt{\tau_0/\rho}[-3.05 + 5.0 \ln((\sqrt{\tau_0/\rho}) \cdot (y/\nu))]$	$D_{\text{turb}} = (((R-r)/5)\sqrt{\tau_0/\rho}) - \nu$	$D_{\text{axial}} = D_{\text{turb}} + D_{\text{mole}}$
Turbulent core area	$y > (30\nu/\sqrt{\tau_0/\rho})$	$u = \sqrt{\tau_0/\rho}[5.5 + 2.5 \ln((\sqrt{\tau_0/\rho}) \cdot (y/\nu))]$	$D_{\text{turb}} = ((R-r)^2/2.5R)\sqrt{\tau_0/\rho}$	$D_{\text{axial}} = D_{\text{turb}}$

effective viscosity. In the mixed segment, the diffusion coefficient is assumed to be related to the concentration and the gradient of the physical properties. Thus, the influence of the difference in density and viscosity on the generation of the contaminated mixing segment is shown in Table 2, where ρ_c and μ_c are the oil density and viscosity of mixed oil; D_{dens} is the diffusion coefficient caused by different density of the oils (m^2/s); D_{visc} is the diffusion coefficient caused by different viscosity of the oils (m^2/s); D_{ρ_0} is the mixture coefficient when the fluids have equal density, which is generally $10^{-2} \sim 10^{-3} \text{ cm}^2/\text{s}$; D_{μ_0} is the mixed coefficient when the fluids have the same viscosity, which is also generally $10^{-2} \sim 10^{-3} \text{ cm}^2/\text{s}$; K_ρ is the proportional constant for density ($\text{m}/(\text{Pa}\cdot\text{s})$); and K_μ is the proportional constant for viscosity ($\text{m}/(\text{Pa}\cdot\text{s})$).

3.3. Adsorption Effects of the Pipe Wall. Because of the roughness of the pipe, the oil molecules will be absorbed in the rough inner surface of the pipe when oil flows and then form a stable adsorption layer because of the action of the molecular force and electrostatic field. A maximum concentration balanced with the component concentration will reach the adsorption layer. The equilibrium adsorption concentration equation, also known as the Langmuir adsorption isotherm [25], is shown as follows:

$$C_r(\infty) = \frac{aC}{1+bC},$$

$$a = \frac{K_a C_r^*}{K_d}, \quad (3)$$

$$b = \frac{K_a}{K_d}.$$

Here, C is the concentration of front oil, C_r is the concentration when the process of the adsorption reaches the balance, K_a is the constant of adsorption (s^{-1}), C_r^* is the extremity adsorption concentration, and K_d is the stripping constant (s^{-1}). The values of a and b are determined as

constants which are associated with temperature and pressure. During the sequence transportation, because the concentration reaching a balanced value C_r in the adsorption layer consumes much shorter time than that required for the concentration variation caused by pipe flow, the adsorption will reach a balance instantly. Thus, the balance concentration C_r can be solved by using the balanced adsorption equation:

$$C_r = \frac{a}{1+bC} C. \quad (4)$$

The derivate dC_r/dC is

$$\frac{dC_r}{dC} = \frac{a}{(1+bC)^2} > 0. \quad (5)$$

When the pipe wall has an adsorption effect on the liquid molecule, the variation of concentration over time is as follows:

$$\frac{\partial C}{\partial t} = \frac{1}{r} \cdot \frac{\partial}{\partial r} \left(r D_{\text{axial}}^{\text{new}} \frac{\partial C}{\partial r} \right) + \frac{\partial}{\partial x} \left(D_{\text{axial}}^{\text{new}} \frac{\partial C}{\partial x} \right) - u \frac{\partial C}{\partial x} - \frac{\partial C_r}{\partial t}. \quad (6)$$

Here, $D_{\text{axial}}^{\text{new}}$ is the new effective axial diffusion coefficient proposed in this paper (m^2/s). u is the velocity of the fluid in the tube, and it is calculated via the formula in Table 1. It is noticed that C and C_r have the same unit. Both of them mean the volume fraction of front oil, and thus, they are both dimensionless. The difference between them is as follows: C is the volume fraction (concentration) of front oil in any controlling volume. C_r means the adsorbed volume fraction of front oil by the wall in the same controlling volume. Thus, C_r is part of C . We define C_r as the concentration when the process of the adsorption reaches the balance. The ‘‘balance’’ means C_r can change in an instant. C_r is only related to parameters a and b as well as C . An increase in C could lead to an increase in C_r .

The right-hand side term $\partial C_r/\partial t$ means ΔC_r has been absorbed by the wall from C during Δt , resulting in part of $\partial C/\partial t$. Meanwhile, ΔC_r means the change of the balanced

TABLE 2: Effects of the difference in density and viscosity of adjacent oils on the diffusion coefficient [23–25].

Effects of different properties	Density difference	Viscosity difference
Assumptions	$D_{\text{dens}} = D_{\rho_0} (1 + K_{\rho} (\partial\rho_c/\partial x))$	$D_{\text{visc}} = D_{\mu_0} (1 + K_{\mu} (\partial\mu_c/\partial x))$
An empirical formula for the density or viscosity of mixed oils	$\rho_c = C\rho_1 + (1 - C)\rho_2$	$\ln \mu_c = C \ln \mu_1 + (1 - C) \ln \mu_2$
Conversion of formulas	$\rho_c = \rho_1 f_{\rho}(C)$ $f_{\rho}(C) = C + (1 - C)(\rho_2/\rho_1)$ $f'_{\rho}(C) = 1 - (\rho_2/\rho_1)$ $(\partial\rho_c/\partial x) = (\partial\rho_c/\partial C) (\partial C/\partial x) = \rho_1 f'_{\rho}(C) (\partial C/\partial x)$ $= \rho_1 (1 - (\rho_2/\rho_1)) (\partial C/\partial x)$	$\mu_c = \mu_1 f_{\mu}(C)$ $f_{\mu}(C) = (\mu_2/\mu_1)^{1-C}$ $f'_{\mu}(C) = -(\mu_2/\mu_1)^{1-C} \ln(\mu_2/\mu_1)$ $(\partial\mu_c/\partial x) = (\partial\mu_c/\partial C) (\partial C/\partial x) = \mu_1 f'_{\mu}(C) (\partial C/\partial x)$ $= \mu_1 (\mu_2/\mu_1)^{1-C} \ln(\mu_2/\mu_1) (\partial C/\partial x)$

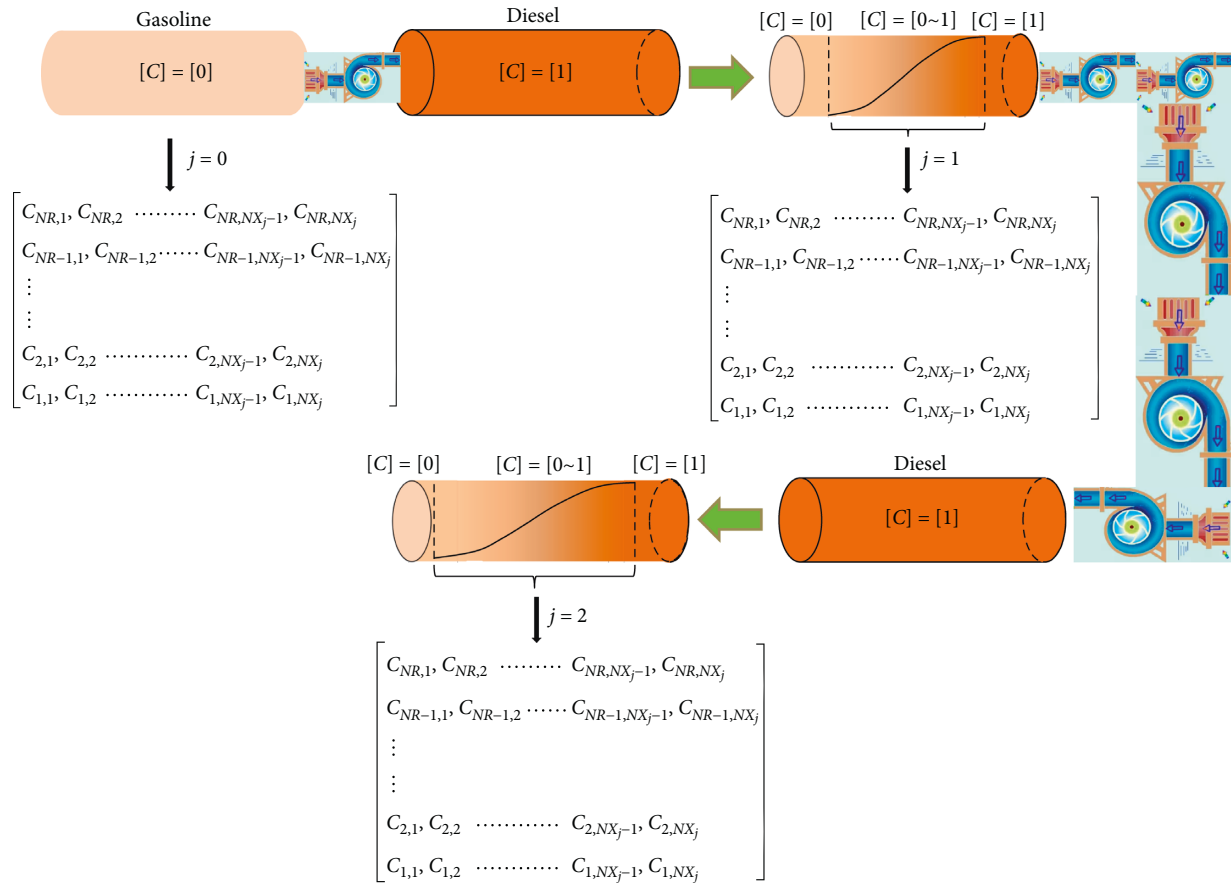


FIGURE 3: Numerical simulation of the movement of a single oil-mixing interface in a long-distance pipeline.

concentration due to the change of a , b , or C in $C_r = (a/(1 + bC))C$.

Also, we have

$$\frac{\partial C_r}{\partial t} = \frac{\partial C_r}{\partial C} \frac{\partial C}{\partial t} = \frac{a}{(1 + bC)^2} \frac{\partial C}{\partial t}. \quad (7)$$

Substituting this into the unsteady convection-diffusion equation, the following is obtained:

$$\left[1 + \frac{a}{(1 + bC)^2} \right] \frac{\partial C}{\partial t} + u \frac{\partial C}{\partial x} = \frac{1}{r} \cdot \frac{\partial}{\partial r} \left(r D_{\text{axial}}^{\text{new}} \frac{\partial C}{\partial r} \right) + \frac{\partial}{\partial x} \left(D_{\text{axial}}^{\text{new}} \frac{\partial C}{\partial x} \right). \quad (8)$$

In this nonlinear partial differential equation, the coefficient of the time term is a second-order variable coefficient which is associated with state variable C leading to hardness in solving the equation. It is noticed that only within the laminar flow layer (near the wall), the

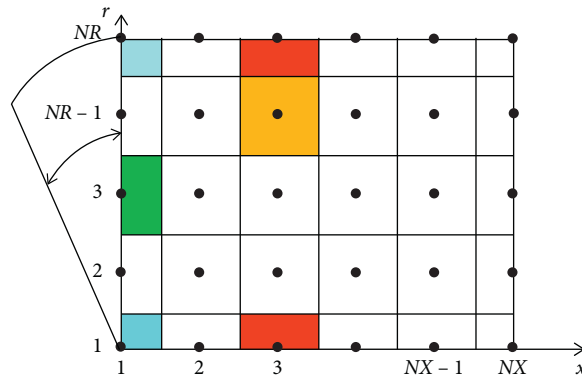


FIGURE 4: Internal node and control volume in a cylindrical coordinate system.

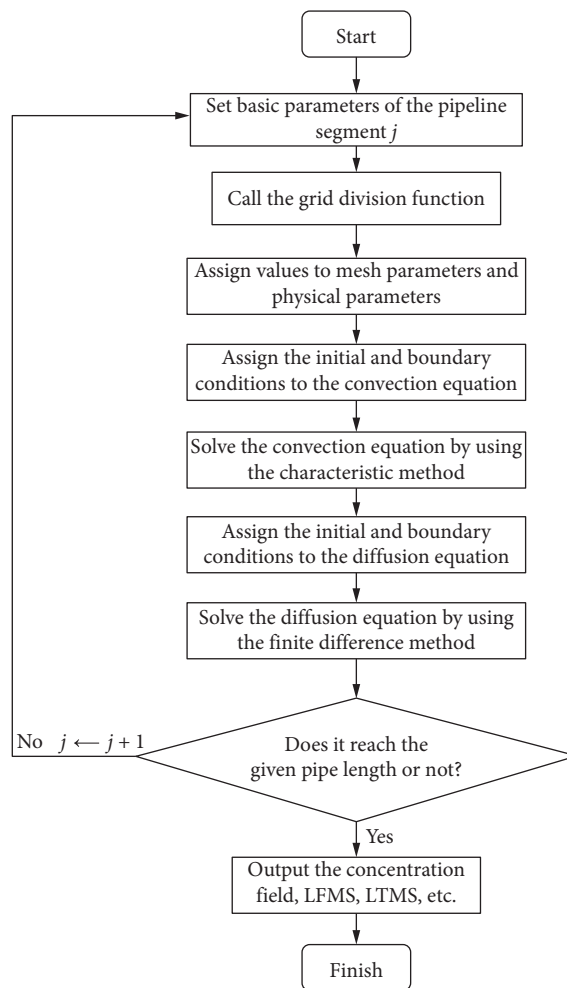


FIGURE 5: Flow chart of the calculation.

parameters a and b have a nonzero value, whereas it is zero as the molecular force and electrostatic field are ineffective.

3.4. Oil-Mixing Model Involving Turbulence Diffusion, the Difference of Physical Properties, and the Effect of Adsorption.

Based on the above contents, a two-dimensional convection-diffusion model considering the difference of physical properties in adjacent oils can be described as follows:

$$\left[1 + \frac{a}{(1 + bC)^2}\right] \frac{\partial C}{\partial t} + u \frac{\partial C}{\partial x} = \frac{1}{r} \cdot \frac{\partial}{\partial r} \left(r D_{\text{axial}}^{\text{new}} \frac{\partial C}{\partial r} \right) + \frac{\partial}{\partial x} \left(D_{\text{axial}}^{\text{new}} \frac{\partial C}{\partial x} \right), \quad (9)$$

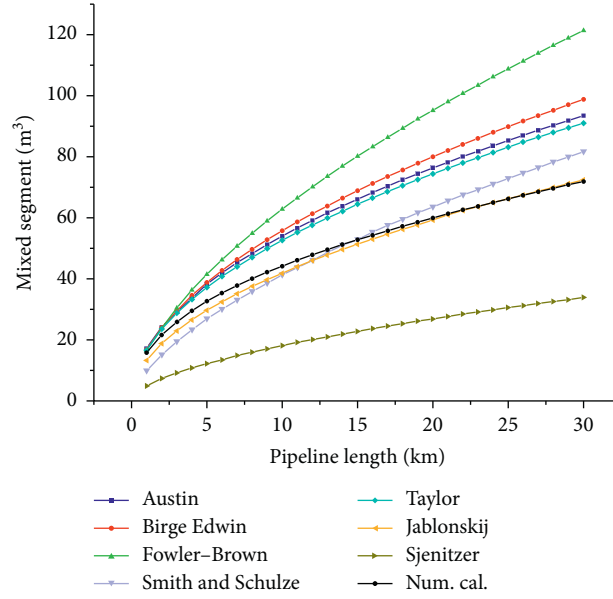


FIGURE 6: Comparison of calculated results to those of empirical formulas.

TABLE 3: Empirical formulas for calculating VMS.

Formula name	Expression
Austin [12]	$(V_m/V_p) = \begin{cases} 18384\sqrt{D/L} \cdot \text{Re}^{-0.9} \cdot e^{2.18\sqrt{D}}, & \text{Re} < \text{Re}_j, \\ 11.75\sqrt{D/L} \cdot \text{Re}^{-0.1}, & \text{Re} > \text{Re}_j \end{cases}$
Birge Edwin [26]	$(V_m/V_p) = (1.4042/D^2 L^{0.471})$
Fowler and Brown [15]	$(V_m/V_p) = 4 \cdot (D/L)^{0.4} \cdot \alpha_1 (N_{\text{Re}}, C)$
Smith and Schulze [16]	$(V_m/V_p) = 4 \cdot (1/L)^{0.38} \cdot ((268.75\text{Re}^{0.13} + 0.1375\text{Re})/\text{Re})$
Taylor [14]	$(V_m/V_p) = 4 \cdot (D/L)^{0.5} \cdot (1/\text{Re})^{0.0625} \cdot (Z)$
Jablonskij [25]	$(V_m/V_p) = 4 \cdot (D/L)^{0.4} \cdot ((6585 + 0.4925\text{Re})/\text{Re}) \cdot ((\sqrt[3]{1/C_1}) - (\sqrt[3]{1/C_2})) \cdot (\rho_1/\rho_2)$ and $V_m/V_p = 4 \cdot (D/L)^{0.5} \cdot ((3000 + 60.7\text{Re}^{0.545})/\text{Re})^{0.5} \cdot (Z)$
Sjenitzer [17]	$(V_m/V_p) = 4 \cdot (D/L)^{0.43} \cdot (37.8/\text{Re}^{0.45}) \cdot (Z)$

in which the new effective axial diffusion coefficient $D_{\text{axial}}^{\text{new}}$ is

$$D_{\text{axial}}^{\text{new}} = \frac{D_{\text{axial}}}{D_{\text{mole}}} (D_{\text{dens}} + D_{\text{visc}})$$

$$= \frac{D_{\text{axial}}}{D_{\text{mole}}} \left\{ D_{\rho_0} \left[1 + K_{\rho} |(\rho_1 - \rho_2)| \left(\left| \frac{\partial C}{\partial x} + \frac{\partial r C}{\partial r} \right| \right) \right] + D_{\mu_0} \left[1 + K_{\mu} \mu_1 \left| \ln \left(\frac{\mu_1}{\mu_2} \right) \right| \left(\frac{\mu_2}{\mu_1} \right)^{1-C} \left(\left| \frac{\partial C}{\partial x} + \frac{\partial r C}{\partial r} \right| \right) \right] \right\}. \quad (10)$$

3.5. Initial Conditions and Boundary Conditions. Definite conditions contain initial conditions and boundary conditions. The concentration of front oil is denoted as C .

Initial conditions [20, 25]:

$$\begin{cases} t = 0, x = 0, C = C_0 = 0.5, \\ t = 0, x > 0, C = 1. \end{cases} \quad (11)$$

Boundary conditions [20, 25]:

$$\begin{cases} t \geq 0, x \rightarrow \infty, C = 1, \\ t \geq 0, \frac{\partial C}{\partial r} \Big|_{r=0} = \frac{\partial C}{\partial r} \Big|_{r=R} = 0, \\ t > 0, x = 0, C = 0. \end{cases} \quad (12)$$

Among them, C_0 is the initial volume concentration of oil B which follows the front oil A (dimensionless), $1 - C$ is the concentration value of subsequent oil (dimensionless), R

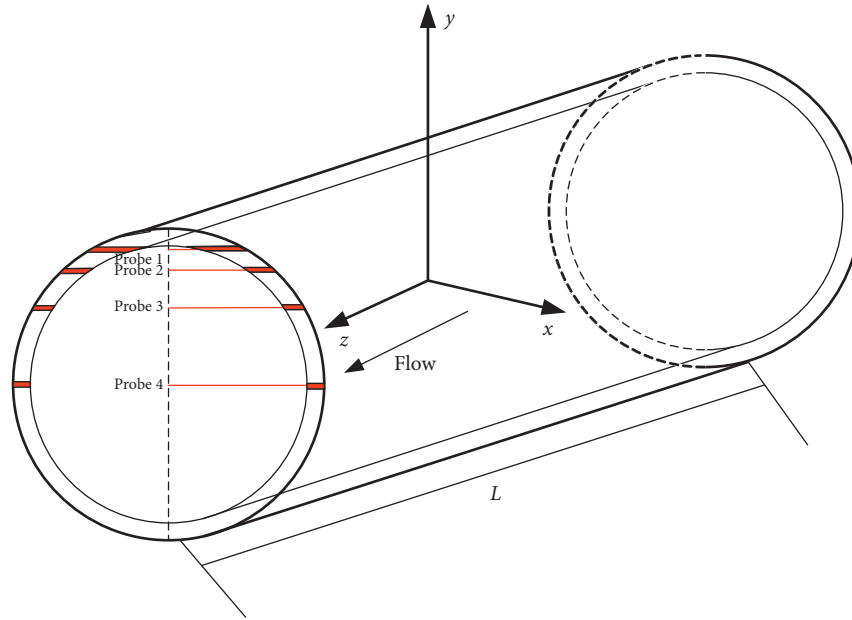


FIGURE 7: Distribution and marking of the probes in the experimental pipe.

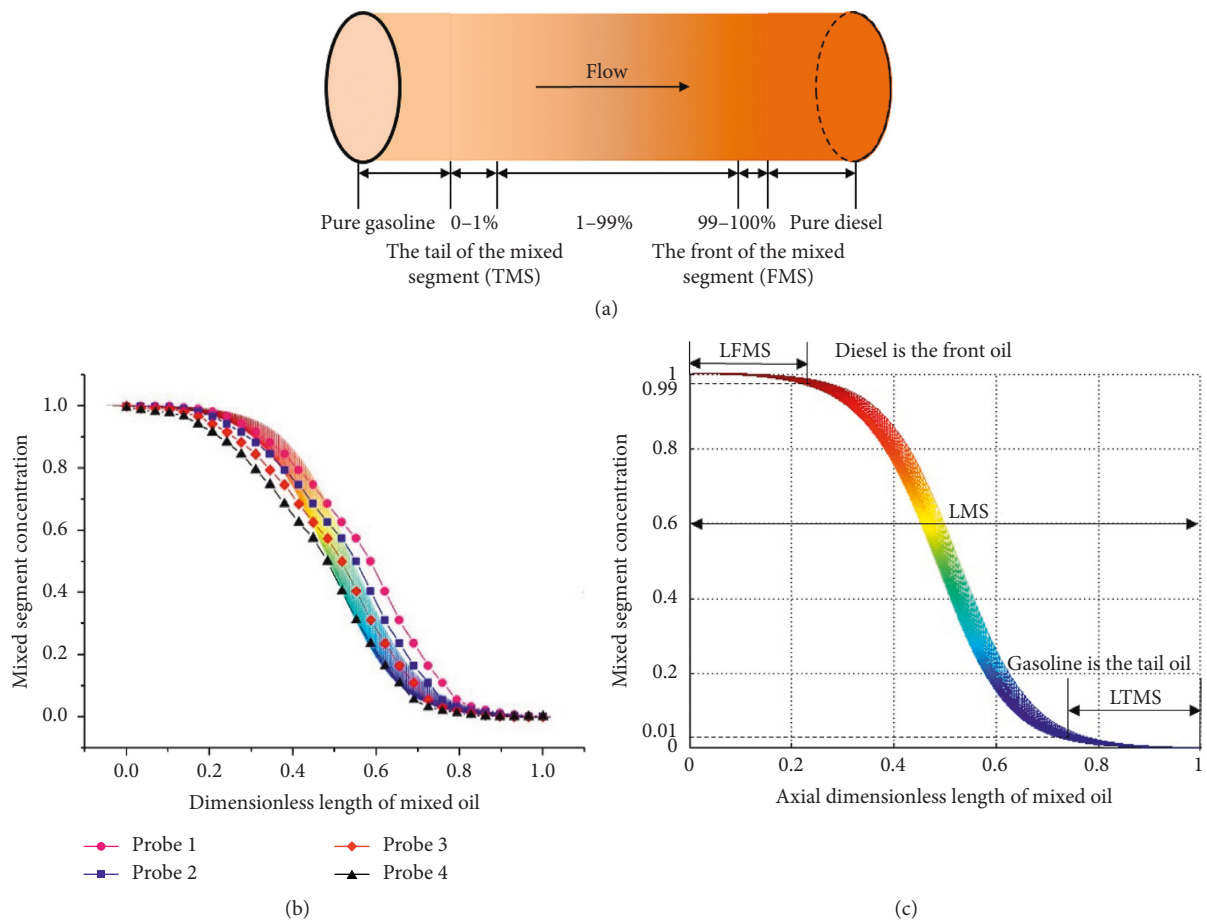


FIGURE 8: Experimental results are compared with the numerical simulation results. (a) Interface distribution in the mixed segment. (b) Re of the experimental result is 33245.7. (c) Re of the numerical simulation result is 33245.7.

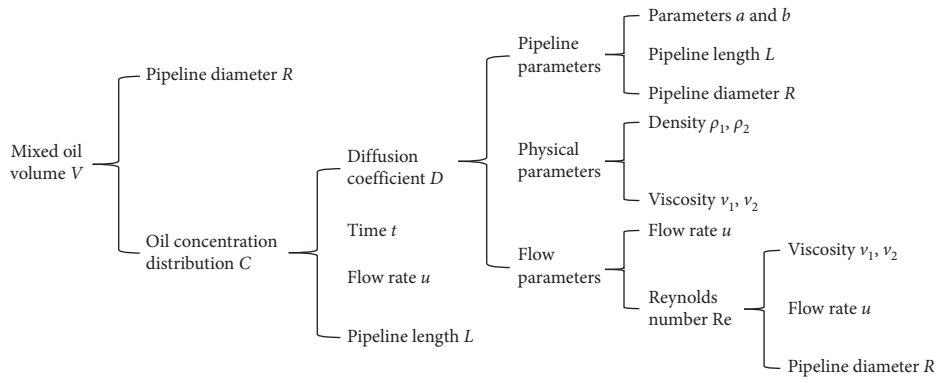


FIGURE 9: Influence factor.

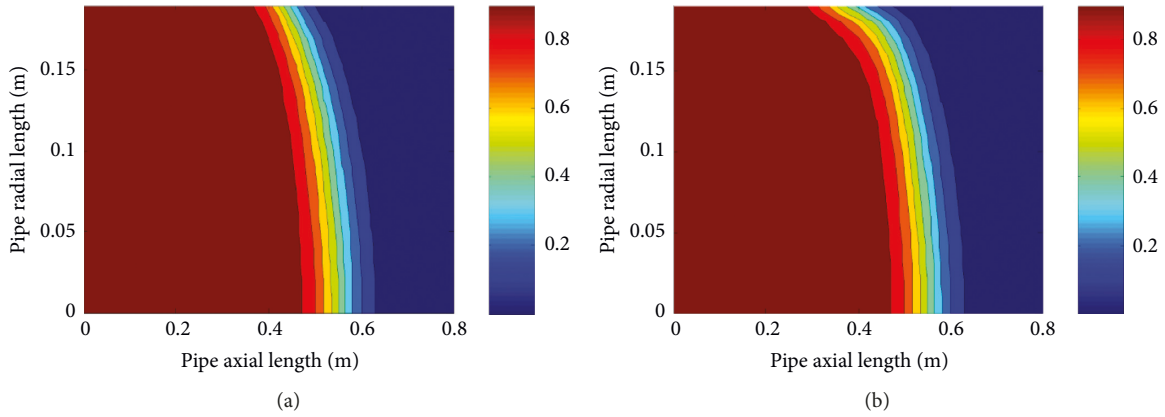


FIGURE 10: CDMS (a) when considering the adsorption effect and (b) without considering the adsorption effect.

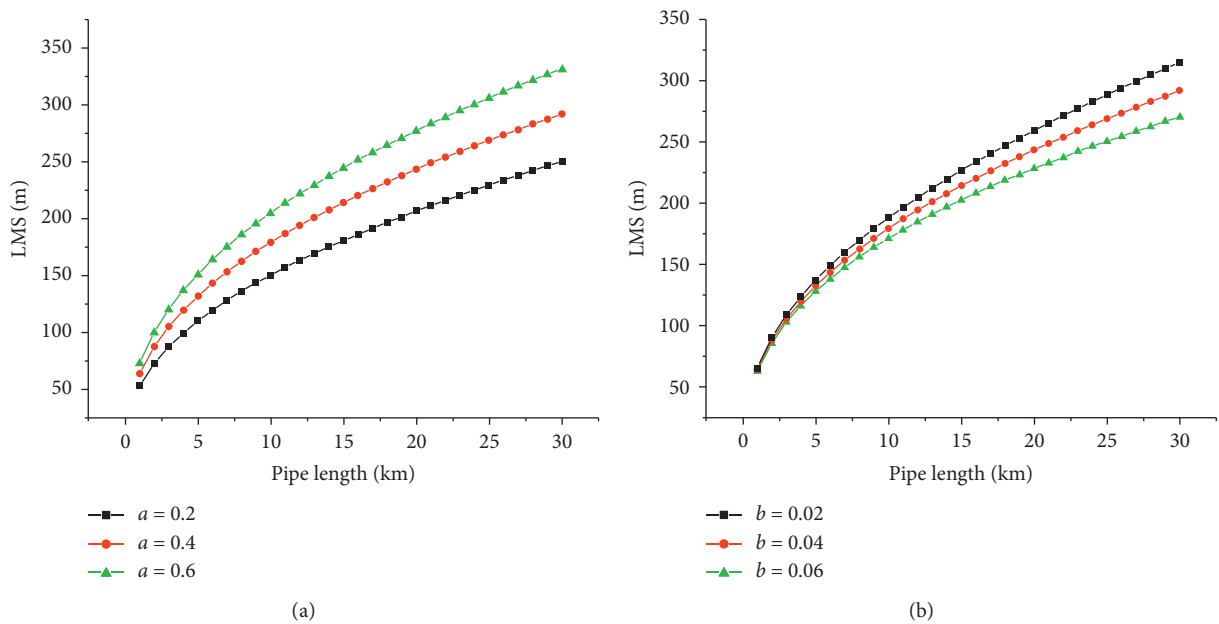


FIGURE 11: Effects of adsorption parameters a (a) and b (b) on LMS.

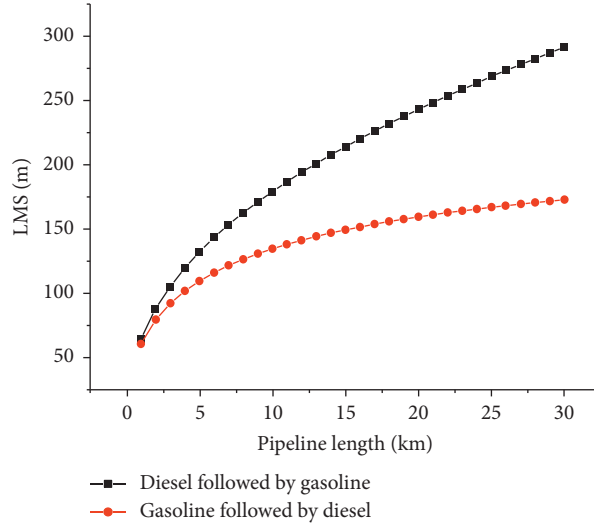


FIGURE 12: Influence of the oil sequence on VMS.

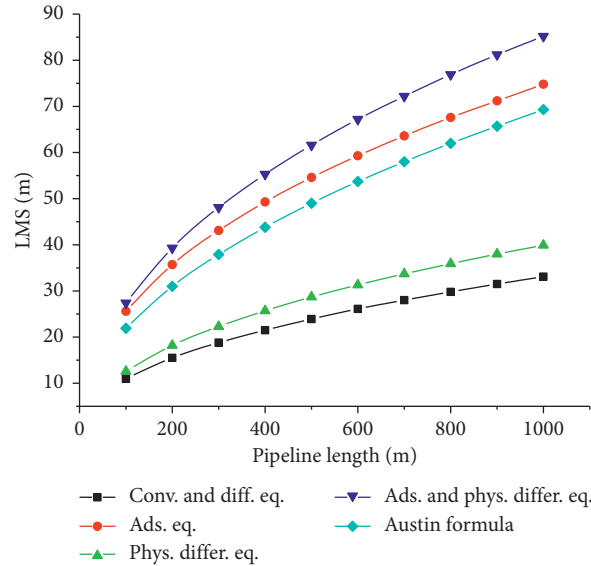


FIGURE 13: Comparison of the adsorption effect and the diffusion coefficient.

is the internal radius of the oil pipeline (m), and x represents the distance between a certain point and the first end of the pipeline (m).

4. Method for Simulating the Growth of Interface in the Long-Distance Pipeline

4.1. The Basic Equation of the Migration of Mixed Oil Segment in Multiple Pipeline Segments. Supposing that the front and tail of the mixed oil segment between two batches are located at S_{front} and S_{tail} , where the location is the function of time and of the pipe segment number that the mixed segment has gone through, we can conclude the basic equation of the migration of $S_{\text{front}}(t, j)$ and $S_{\text{tail}}(t, j)$ is shown as equation (13). Here, the function $u(t)$ in $u(t, S_{\text{front}}(t, j))$ means convection of S , while $u(S_{\text{front}}(t, j))$ in $u(t, S_{\text{front}}(t, j))$ means other performances of S such as diffusion and wall adsorption. These performances could

make S grow on the basis of its current state, resulting in the velocity u being related to current S . In other words, S flows and grows:

$$\frac{\partial S_{\text{front}}(t, j)}{\partial t} = u(t, S_{\text{front}}(t, j)), \quad j = 1, 2, \dots, N, \quad (13)$$

$$\frac{\partial S_{\text{tail}}(t, j)}{\partial t} = u(t, S_{\text{tail}}(t, j)), \quad j = 1, 2, \dots, N,$$

where t is the time (s); $S_{\text{front}}(t, j)$ and $S_{\text{tail}}(t, j)$ are the position of the front and tail of the mixed oil segment, respectively (m); N is the total number of the pipe segments (dimensionless); j is the numbering of the pipe segment arranged from small to large according to the distance from the inlet (dimensionless); and u is the average cross-sectional velocity of the fluid (m/s).

Because of $0 \leq L_j \leq S_{\text{tail}}(t, j) \leq S_{\text{front}}(t, j) < L_{j+1}$, we have the following boundary conditions:

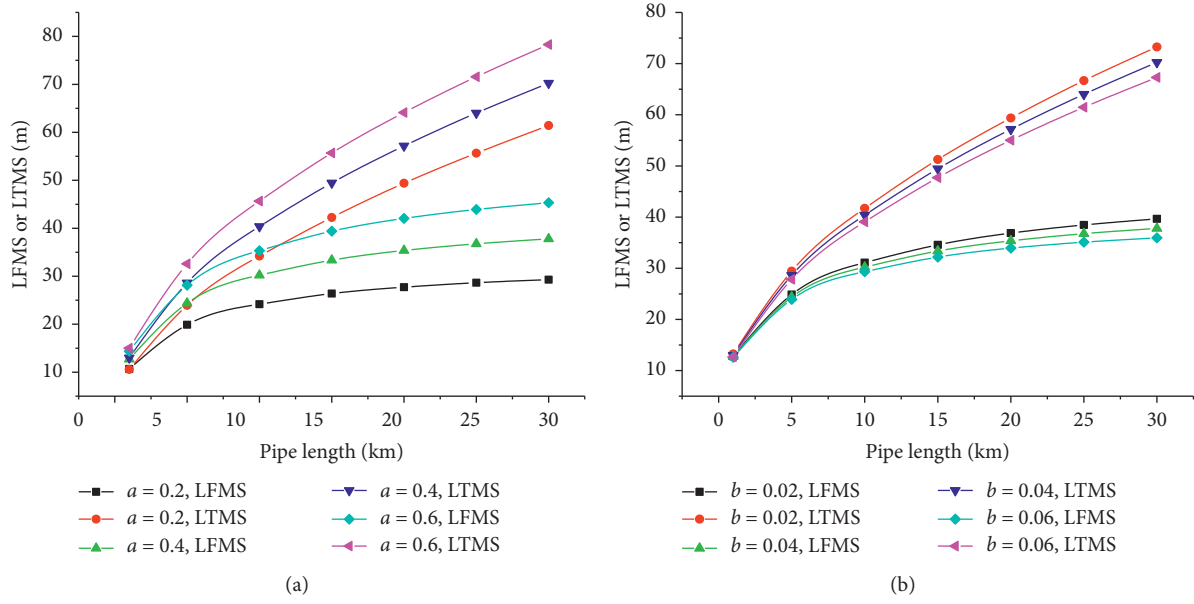


FIGURE 14: Effects of parameters a (a) and b (b) on LFMS and LTMS.

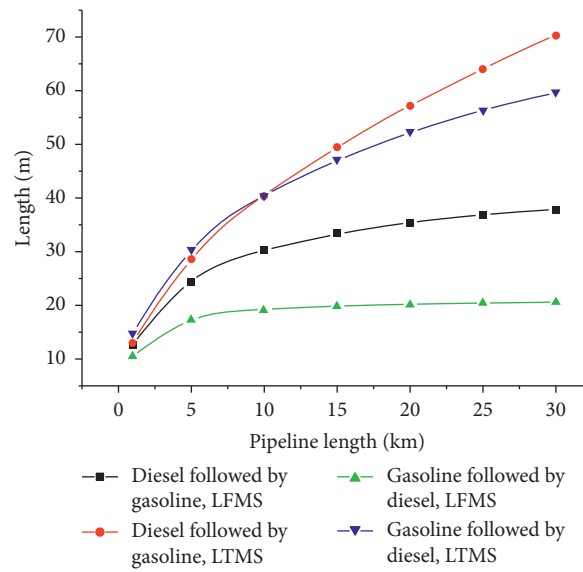


FIGURE 15: Effects of oil properties on LTMS.

$$\begin{cases} u(t, 0) = u_{\text{inlet}}(t), \\ u(t, L_{\text{pipe}}) = u_{\text{outlet}}(t), \\ S_{\text{front}}(t, 0) = S_{\text{tail}}(t, 0) = 0, \\ S_{\text{front}}(t, N) > S_{\text{tail}}(t, N) \geq L_{\text{pipe}}, \\ S_{\text{tail}}(t, j) < S_{\text{front}}(t, j), \quad j = 1, 2, \dots, N. \end{cases} \quad (14)$$

The initial conditions are

$$\begin{cases} u(0, x) = u_{\text{init}}, & 0 \leq x \leq L_{\text{pipe}}, \\ S(0, j) = S_{\text{init}} = 0, & 0 \leq j \leq N. \end{cases} \quad (15)$$

At $j = 1$, as can be seen in Figure 3, pure gasoline enters the pipe segment filled with pure diesel to perform the sequential transportation, and thus, the mixed oil segment is

formed. The pure gasoline segment is represented by a matrix with 0, while the mixed segment is represented by a matrix with 0~1. Then, the mixed segment enters the pipe segment with pure diesel and consequently forms a mixed oil segment again, which is numbered as $j = 2$. In this way, the pipe is divided into many segments with different length, and the numerical simulation of the movement of a single oil-mixing interface in a long-distance pipeline can be realized.

In this paper, the internal node method is adopted for the solution, and the distribution relationship between nodes and control volume is shown in Figure 4. In the cylindrical coordinate system, the node distribution on the axial section of the pipeline is shown in Figure 4.

The fractional step method is applied to solve this problem [21] in order to improve the stability of the solution

process. Δt is divided into two parts in each time step. In the former part, the diffusion term is treated as a constant, and the pure convection equation is solved by the characteristic line method. In contrast, in the latter part, the convection term is regarded as a constant, and the finite difference method is used to solve the pure diffusion equation. Figure 5 shows the flow chart of the calculation.

5. Results and Discussion

5.1. Verification of Simulation Results

5.1.1. Comparison of the Simulation Results with the Empirical Formula. The numerical simulation results are compared with the empirical formula under the same conditions. A 30 km pipeline was simulated with the 0# diesel as front oil and the 90# gasoline as tail oil. The temperature is 20°C, and the pipe diameter is 560 mm. The average flow velocity is 1.14 m/s. The mixed oil volume obtained from empirical formulas and numerical simulation results were compared.

As can be seen in Figure 6, with the increase of pipeline length, the increasing rate of the mixed segment gradually slows down. The increasing trend of the mixed segment calculated by numerical simulation is the same as that calculated by other empirical formulas.

In Table 3, V_m is the mixed oil volume (m^3); V_p is the pipeline volume (m^3); D is the diameter of the pipeline (m); L is the length of the pipeline (m); $\alpha_1(N_{Re}, C)$ is the Fowler and Brown [15] experimental constant; Re is the Reynolds number; Re_c is the critical Re ; ρ_1 and ρ_2 are the density of front oil and tail oil, respectively; C_1 and C_2 are the concentration of front oil and tail oil, respectively (100%); and Z is a function of C_1 and C_2 (dimensionless).

The comparisons of LMS results obtained from numerical simulation to others such as Austin and Palfrey [12] empirical formulas (all the equations are shown in Table 3) are shown in Figure 6. The numerical data are in the middle of the results obtained from the empirical formulas, which are larger than the results of Sjenitzer [17] and smaller than the results of Fowler and Brown [15], Birge Edwin [26], Austin and Palfrey [12], and Taylor [14]. The numerical simulation results intersect with those of Smith and Schulze [16] and Jablonskij [25].

5.1.2. Comparison of the Simulation Results with the Experimental Data. We have compared the numerical simulation results to the experimental results under the same conditions. The total length of the experimental pipeline is 200 m, made of plexiglass. The pipe diameter is DN25, and the probe position of the interface detector is shown in Figure 7. The Re of 33245.7 was simulated, and the simulation results were compared to the experimental results. The comparison results are shown in Figure 8.

In Figure 8, under the condition of Re 33245.7, the simulated result is similar to the shape of the mixed segment concentration curve of the experimental result. The simulation results can reflect the concentration difference in the radial direction of the pipe. The first 99-100% of the mixed

segment is the front oil which is mainly diesel, and the last 0-1% of MS is the tail oil which is mainly gasoline.

5.2. Sensitivity Analysis of the Mixed Segment

5.2.1. Influence of the Basic Parameters on the Mixed Segment. In the process of calculating the mixed segment, the influence of various parameters on the mixed segment is shown in Figure 9. When the adsorption effect between the oil and the pipe wall is taken into account, the parameters a and b also become the influencing factors. The following analysis is focused on the adsorption effect and physical differences in the mixed segment.

5.2.2. Adsorption Effect on MS. The comparison between the adsorption effect and the nonadsorption effect is shown in Figure 10, which shows the effect of adsorption on oil concentration. Figure 10(a) shows the simulation result without considering the pipe wall adsorption model, while Figure 10(b) shows the simulation result considering the adsorption effect.

It can be seen from the figure that when considering the adsorption effect, it has little influence on CDMS at the center of the pipe, but it has a significant influence on the oil substitution near the pipe wall. When the adsorption effect is taken into account, the oil concentration gradient at the pipe wall is larger than that without adsorption effect. The adsorption effect results in front oil adhering to the pipe wall, which slows down the oil replacement.

The influence of adsorption parameters a and b on LMS is shown in Figure 11. The influence of a on VMS is positive. When other factors remain unchanged, LMS increases with the increasing a . When a increases by 50.0%, VMS increases by about 14%. The influence of b on VMS is negative. When other factors remain unchanged, LMS decreases with the increasing b . The influence of b on LMS increases with the increasing operating length. When the operating distance is 10 km, b increases by 50.0% and VMS decreases by about 5%. When the operating distance is 20 km, b increases by 50.0% and VMS decreases by about 6%. When the operating distance is 30 km, b increases by 50.0% and VMS decreases by about 7%. When the values of a and b are 0.4 and 0.04, respectively, VMS increases by about 4% compared with that with no adsorption effect.

5.2.3. Effects of Physical Property Difference on MS. Essentially, the diffusion is caused by a concentration gradient, and the diffusion rate is proportional to the concentration gradient of the material. The diffusion coefficient is related to the density, viscosity, and concentration gradient of the oils. The larger the concentration gradient is at a certain position in MS, the larger the corresponding diffusion coefficient value will be, which is in accordance with the nature of the diffusion phenomenon and has a clearer physical significance.

VMS is related to the value of the diffusion coefficient. The model in this paper can reflect the physical properties of

oil and the influence of the concentration gradient on the diffusion coefficient and further reflect the influence of the oil transportation sequence on VMS. The influence of oil sequence exchange on MS is shown in Figure 12. LMS of diesel followed by gasoline is larger than that of gasoline followed by diesel, while both of them are increasing with the transportation distance.

5.2.4. Comparison of the Adsorption Effect and the Diffusion Coefficient. It can be seen from Figure 13 that both the physical property difference of oils and the adsorption effect have a greater influence on LMS than the traditional convection and diffusion processes. The adsorption effect also has a greater influence than the physical property difference of oils on LMS. The result of the Austin formula is between that of the adsorption effect model and that of the physical property difference model. When solving the convection-diffusion equation, if the value of the diffusion coefficient is calculated by the existing empirical formula, the numerical results are quite different from those of the Austin formula. LMS calculated by the improved model is more similar to that calculated by the Austin formula.

5.3. Sensitivity Analysis of the Tailing Phenomenon in the Mixed Segment

5.3.1. Effects of Adsorption on the Tailing Phenomenon. In this paper, the segment with 95–99.9% of front oil concentration is used as LFMS and the segment with 0.1–5% is used as LTMS. Figure 14 shows the influence of adsorption parameters a and b on LTMS. As can be seen from the figure, parameters a and b have an influence on both LFMS and LTMS, where there is a greater influence on LTMS. Both LFMS and LTMS increase with the increasing a and decrease with the increase of b . The influence of a is greater than that of b .

5.3.2. Effects of Different Physical Properties on LTMS. LMS will change when the sequence of oil transportation is changed. As can be seen from Figure 15, the sequence of oil transportation has an impact on LFMS and LTMS. When diesel is the front oil, LFMS and LTMS are longer than those of gasoline being the front oil. The influence of the transportation sequence on LFMS is greater than that on LTMS, but in both cases, LTMS is greater than LFMS. When diesel is followed by gasoline, DBFT is smaller than that in the case when gasoline is followed by diesel.

6. Conclusion

Compared to previous studies, a new method for calculating CDMS is proposed via analyzing the tailing phenomenon of the mixed oil segment in situ, where a new model is proposed to calculate the axial diffusion coefficient by considering the difference in physical properties and turbulence effect. Meanwhile, the pipe wall roughness is involved to process the pipe wall adsorption effect on oil molecules. Based on the new method, LFMS, LTMS, and CDMS are related to the adsorption effect and to the value of the diffusion coefficient,

which is a function of oil density, viscosity, and concentration gradient. The conclusions are summarized as follows:

- (1) The larger the concentration gradient is in a certain part of the mixed segment, the larger the diffusion coefficient value will be.
- (2) The sequence of oil product transportation shows an effect on LFMS and LTMS and shows a greater effect on LFMS. LTMS is always greater than LFMS, no matter what sequence is used. When diesel is followed by gasoline, LMS is larger than that of gasoline followed by diesel, and LFMS and LTMS are also larger.
- (3) When diesel is followed by gasoline, the difference between LFMS and LTMS is rather small and is also smaller than those of gasoline followed by diesel.
- (4) When the adsorption effect on CDMS is simulated, the mixed segment increases with the increasing a . LMS decreases with the increasing b . Both a and b have an influence on LFMS and LTMS, but they have a greater influence on LTMS, and a shows a greater influence than b .
- (5) The simulation results show that the novel model can well describe the mixed segment tailing phenomenon of LTMS and also explain the mixing essence of two miscible but dissimilar fluids in pipelines more clearly. To sum up, this model can provide theoretical guidance for the prediction of CDMS and cutting process in practical operation processes; therefore, more economic benefit can be obtained.

Abbreviations

MBDF:	Miscible but dissimilar fluids
MMBDF:	Mixing of miscible but dissimilar fluids
MS:	The mixed segment
LMS:	The length of the mixed segment
VMS:	The volume of mixed oil
LTMS:	The length of the tail of the mixed segment
LFMS:	The length of the front of the mixed segment
CDMS:	The concentration distribution in the mixed segment
DBFT:	The difference between LTMS and LFMS.

Data Availability

The datasets generated and/or analyzed during the current study are available from the corresponding author on reasonable request.

Conflicts of Interest

The authors declare that there are no conflicts of interest regarding the publication of this paper.

Acknowledgments

This work was funded by the China Postdoctoral Science Foundation (2019M653481) and by the National Natural Science Foundation of China (51674212).

References

- [1] J. Gong, D. F. Yan, and Z. L. Kang, "Research on contamination caused by the topographical difference in batch transportation," in *Proceedings of the 2004 International Pipeline Conference*, vol. 3, pp. 2171–2176, Calgary, Canada, October 2004.
- [2] Z. L. Kang, J. Gong, and D. F. Yan, "Development of model for contaminated oil product caused by elevation difference in multiproduct pipelines," *Journal of China University of Petroleum*, vol. 27, pp. 65–67, 2003.
- [3] A. R. Patrachari and A. H. Johannes, "A conceptual framework to model interfacial contamination in multiproduct petroleum pipelines," *International Journal of Heat and Mass Transfer*, vol. 55, no. 17–18, pp. 4613–4620, 2012.
- [4] J. Gong, Q. Wang, W. Wang, and Y. Guo, "The calculation method of mixing volume in a products pipeline," in *Proceedings of the 2010 8th International Pipeline Conference*, vol. 3, pp. 393–398, Calgary, Canada, September 2010.
- [5] S. R. D. Melo and F. B. F. Rachid, "Computing transmit in complex batch transfers via the mixing-volume-equivalent-pipe concept," *International Pipeline Conference*, vol. 3, pp. 605–610, 2010.
- [6] E. S. Udoetok and A. N. Nguyen, "A disc pig model for estimating the mixing volumes between product batches in multi-product pipelines," *Journal of Pipeline Engineering*, vol. 8, no. 3, pp. 195–204, 2009.
- [7] D. C. Cafaro and J. Cerdá, "A rigorous mathematical formulation for the scheduling of tree-structure pipeline networks," *Industrial and Engineering Chemistry Research*, vol. 50, no. 9, pp. 5064–5085, 2010.
- [8] F. B. Freitas, J. H. Carneiro de Araujo, and R. M. Baptista, "Predicting mixing volumes in serial transport in pipelines," *Journal of Fluids Engineering*, vol. 124, no. 2, pp. 528–534, 2002.
- [9] D. A. Rodríguez, P. P. Oteiza, and N. B. Brignole, "Simulated annealing optimization for hydrocarbon pipeline networks," *Industrial and Engineering Chemistry Research*, vol. 52, no. 25, pp. 8579–8588, 2013.
- [10] G. He, Y. Liang, Y. Li et al., "A method for simulating the entire leaking process and calculating the liquid leakage volume of a damaged pressurized pipeline," *Journal of Hazardous Materials*, vol. 332, pp. 19–32, 2017.
- [11] Z. Pan, B. Chen, L. Shang, and Y. Yan, "Pressure loss and energy consumption of an inner-cone flowmeter and orifice plate flowmeter in the product pipeline," *Energy Sources, Part A: Recovery, Utilization, and Environmental Effects*, vol. 33, no. 4, pp. 370–376, 2010.
- [12] J. E. Austin and J. R. Palfrey, "Mixing of miscible but dissimilar liquids in serial flow in a pipeline," *ARCHIVE: Proceedings of the Institution of Mechanical Engineers*, vol. 178, no. 1, pp. 377–395, 1963.
- [13] Z. Aunicky, "The longitudinal mixing of liquids flowing successively in pipelines," *The Canadian Journal of Chemical Engineering*, vol. 48, no. 1, pp. 12–16, 1970.
- [14] G. Taylor, "The dispersion of matter in turbulent flow through a pipe," *Proceedings of the Royal Society of London. Series A. Mathematical and Physical Sciences*, vol. 223, no. 1155, pp. 446–468, 1954.
- [15] F. C. Fowler and G. G. Brown, *Contamination by Successive Flow in Pipe Lines*, American Institute of Chemical Engineers, New York, NY, USA, 1943.
- [16] S. S. Smith and R. K. Schulze, "Interfacial mixing characteristics of products in products pipe line-Part 1," *The Petroleum Engineer*, vol. 20, no. 8, 1948.
- [17] F. Sjenitzer, "How much do products mix in a pipeline; here is how to calculate the extent of contamination when two different liquids are pumped in succession," *Pipeline Engineer*, vol. 30, pp. 31–34, 1958.
- [18] L. J. Tichacek, C. H. Barkeley, and T. Baron, "Axial mixing in pipes," *American Institute of Chemical Engineers Journal*, vol. 3, no. 4, pp. 439–442, 1957.
- [19] D. Shongsheng and P. Jianing, "The comparison of mixing models of two-D products batching," *Oil and Gas Journal*, vol. 1, pp. 16–18, 1997.
- [20] D. Shongsheng and P. Jianing, "Application of convection diffusion equation to the analysis of contamination between batches in multiproduct pipeline transport," *Applied Mathematics and Mechanics*, vol. 19, no. 8, pp. 50–57, 1998.
- [21] Z. Y. Xia and Q. Q. Liu, "Numerical simulation of the contamination between batches in multi-product pipeline transport," *Mechanics in Engineering*, vol. 6, pp. 10–15, 2010.
- [22] M. B. Lulie, *Optimization of Multi-Products Pipeline*, Vol. 18, Chinese Petroleum Industry Press, Beijing, China, 1989.
- [23] H. Mostafaei, P. M. Castro, and A. Ghaffari-Hadigheh, "A novel monolithic MILP framework for lot-sizing and scheduling of multiproduct treelike pipeline networks," *Industrial and Engineering Chemistry Research*, vol. 54, no. 37, pp. 9202–9221, 2015.
- [24] H. Shahandeh and Z. Li, "Modeling and optimization of the upgrading and blending operations of oil sands bitumen," *Energy and Fuels*, vol. 30, no. 7, pp. 5202–5213, 2016.
- [25] G. He, M. Lin, B. Wang, Y. Liang, and Q. Huang, "Experimental and numerical research on the axial and radial concentration distribution feature of miscible fluid interfacial mixing process in products pipeline for industrial applications," *International Journal of Heat and Mass Transfer*, vol. 127, pp. 728–745, 2018.
- [26] S. Chintala, "Computational study of interfacial mixing in pipelines, logistics and diverse models to predict the interface length," pp. 67–69, Doctoral dissertation, Oklahoma State University, Stillwater, OK, USA, 2014.

